Electronic Supplementary Information for

Where is the best substitution position for amino groups on carbon dots: a computational strategy toward long-wavelength red emission

Nengjie Cao,[1,2] *Quan Wang,*[1,2] *Xianggui Zhou,*[3] *Yixun Gao,*[1,2] *Yancong Feng,*[*,1,2]

Hao Li,[1,2] *Pengfei Bai,*[1,2] *Yao Wang,*[*,1,2] and *Guofu Zhou*[1,2]

[1]Guangdong Provincial Key Laboratory of Optical Information Materials and Technology & Institute of Electronic Paper Displays, South China Academy of Advanced Optoelectronics, South China Normal University, Guangzhou 510006, P. R. China

[2]National Center for International Research on Green Optoelectronics, South China Normal University, Guangzhou 510006, P. R. China

[3]School of Chemistry, South China Normal University, Guangzhou 510006, P. R. China

Corresponding Author: Yancong Feng E-mail: fengyancong@m.scnu.edu.cn

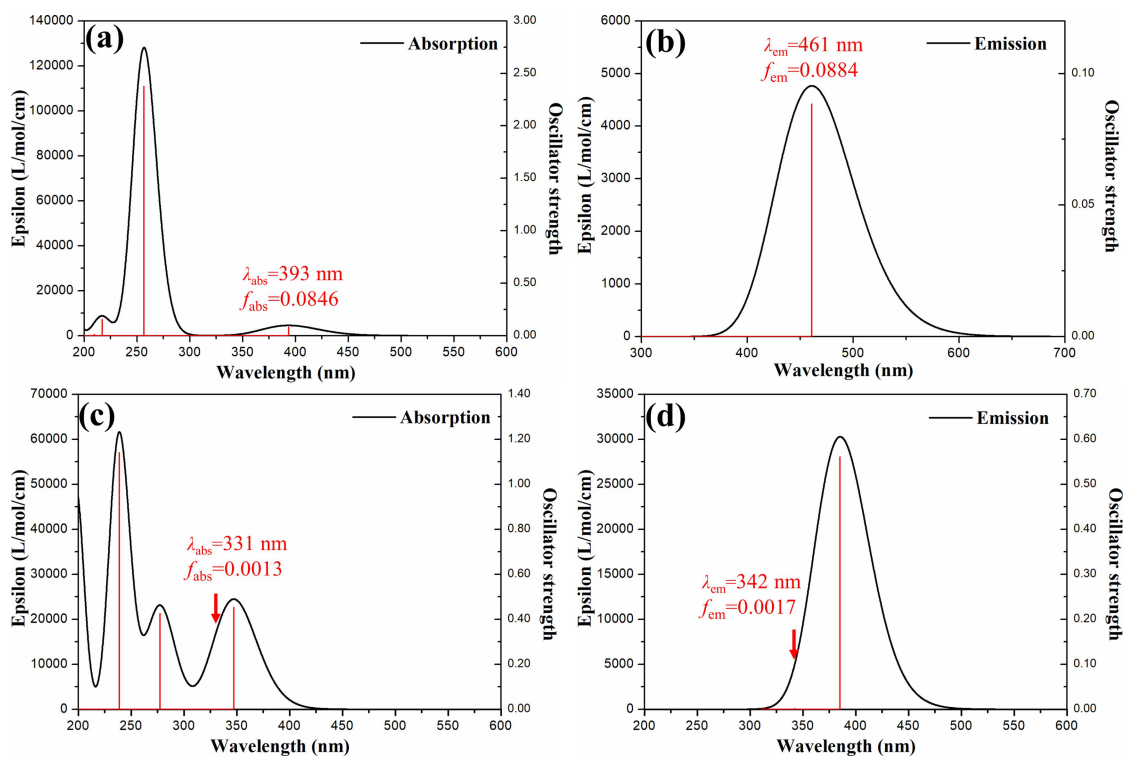*Yao Wang E-mail*: wangyao@m.scnu.edu.cn

Figure S1. Absorption and emission spectra of (a, b) unsubstituted anthracene and (c, d) pyrene (FWHM=0.5 eV).
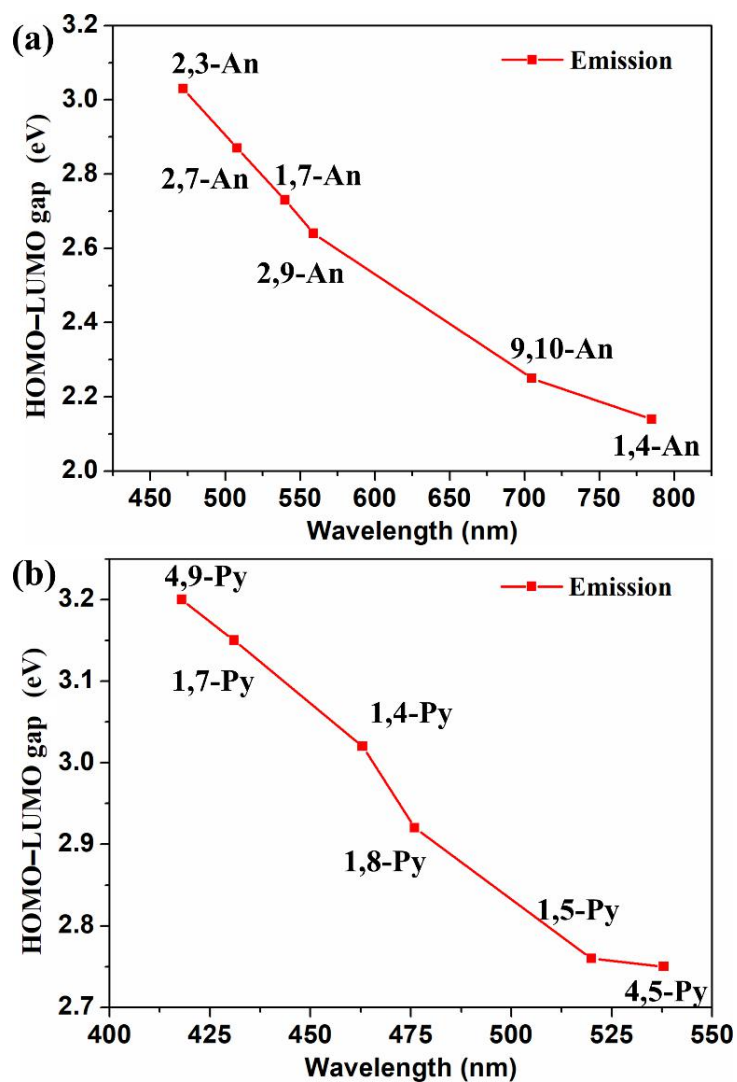
Figure S2. Correlation maps of HOMO−LUMO gap and emission wavelength of CDs:

(a) anthracene and (b) pyrene.

The "hole & electron" maps of Figure S3 show that the hole (electron depletion) of 1,4-An with the longest wavelength emission mainly concentrates on amino groups part, and 1,4-An has the largest hole contribution value (see the data of Table 1 calculated via "Equations"). Further, the "C_{hole} & C_{ele}" maps show that 1,4-An has the largest charge transfer distance (D). The electron separation degree (t) value of 1,4-An is the largest value, i.e., 0.95, indicating that the charge separation of 1,4-An is quite sufficient. The large positive values show that the hole and electron separation degree are sufficient separation. Moreover, as can be seen in the Table 1, the overlap degree of hole-electron distribution (S_r) and exciton binding energy (E_c) of 1,4-An has the minimum value, further proving the largest charge transfer. The pyrene-based amino-substituted CDs have a similar conclusion as shown in Figure S4. These results show that the large charge transfer from amino groups to CDs core can make PL spectra shift to a long wavelength.

For the local excitation, there is no obvious variety in the distribution area of electrons or its distribution range covers the entire system after the electron are excited.[1] In general, the D index is small, S_r index is large, the t index is obviously negative, and the $\Delta\sigma$ index is small. The main distribution ranges of the excited hole and electron are very close, and the degree of overlap is large. The distributions of hole and electron are not significantly separated, and the distribution widths are similar. For the charge transfer excitation, the distribution area shifts significantly after the electrons are excited.[2]

Figure S3. Plots of "hole" (blue part) and "electron" (green part) (isovalue=0.04), "C_{hole}" (purple part) and "C_{ele}" (green part) by the smooth description, and overlap degree of hole-electron distribution (S_r) (green part) of 2,3-An, 2,7-An, 1,7-An, 2,9-An, 9,10-An, and 1,4-An. The separated distance between hole centroid (purple) and electron centroid (yellow) is the charge transfer distance (*D*).
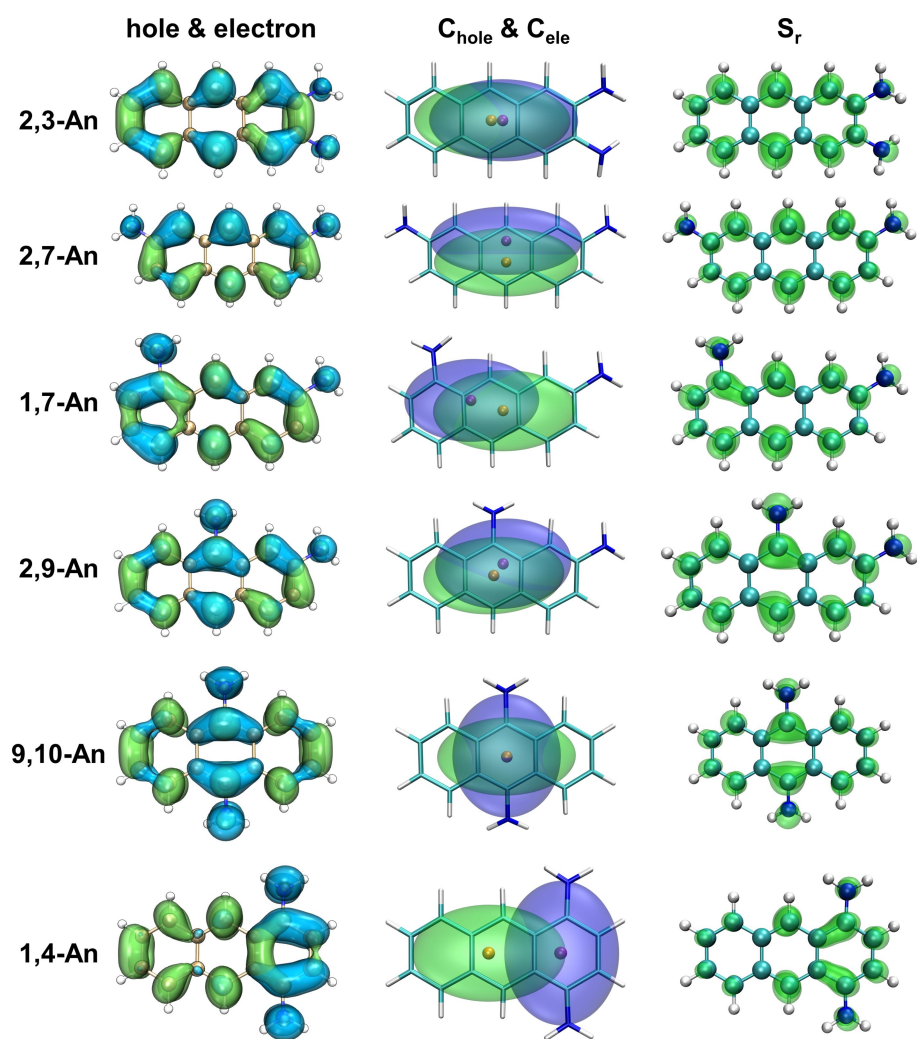
Figure S4. Plots of "hole" (blue part) and "electron" (green part) (isovalue=0.04), "C_{hole}" (purple part) and "C_{ele}" (green part) by the smooth description, and overlap degree of hole-electron distribution (S_r) (green part) of 4,9-Py, 1,7-Py, 1,4-Py, 1,8-Py, 1,5-Py, and 4,5-Py. The separated distance between hole centroid (purple) and electron centroid (yellow) is the charge transfer distance (*D*).
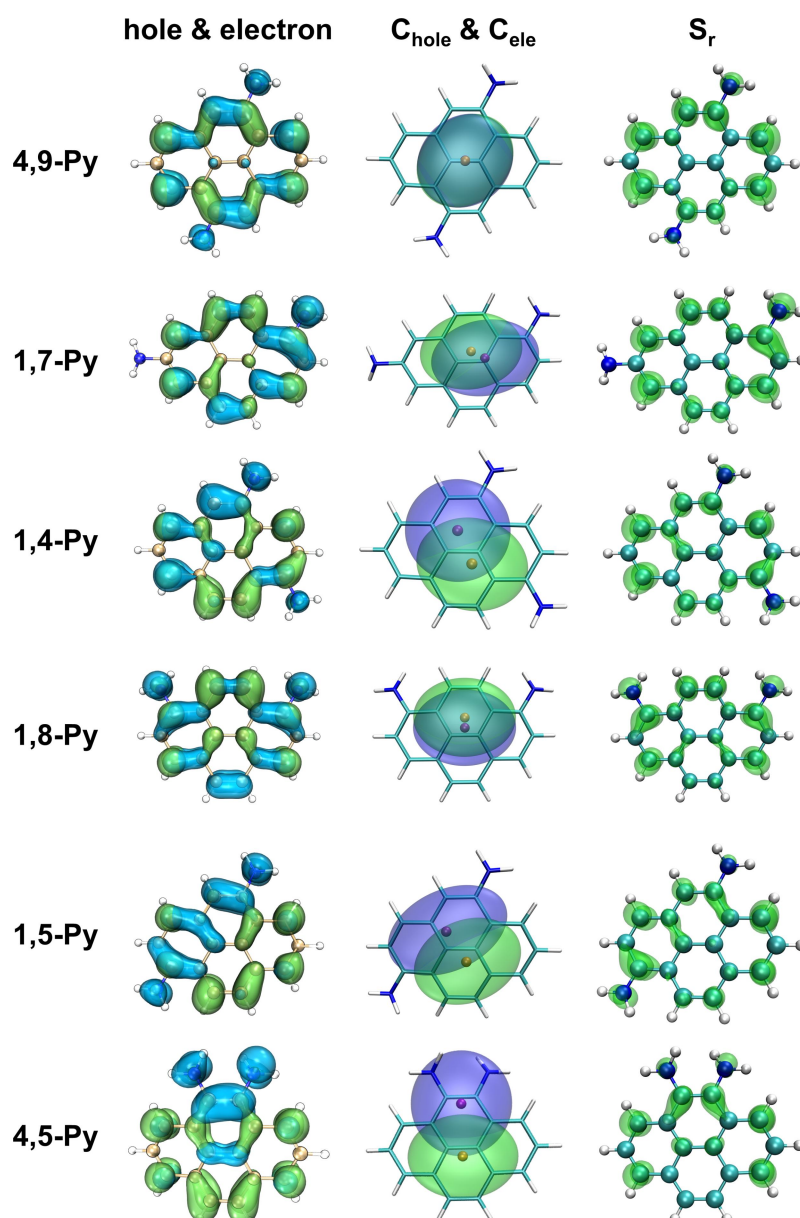
Table S1. Absorption wavelength (λ_{abs} in nm), oscillator strength (f_{abs}), and configuration interaction (CI) contributions (Major MO Involvement, %)[a] of anthracene-based of diamino-substituted CDs shown in Figure 1.

model	λ_{abs}	f_{abs}	CI contribution (%)
2,3-An	408	0.0541	H → L (98.5)
	354	0.2028	H-1 → L (78.3), H → L+1 (20.9)
	278	1.8422	H → L+1 (72.5), H-1 → L (21.1)
	248	0.1679	H-1 → L+1 (95.9)
	240	0.0593	H → L+4 (82.5)
	237	0.5197	H-3 → L (69.1), H → L+4 (13.0)
2,7-An	423	0.0436	H → L (99.1)
	364	0.1917	H-1 → L (79.7), H → L+1 (17.7)
	296	0.9213	H → L+1 (67.2), H-3 → L (14.0), H-1 → L (13.5)
	272	0.4496	H → L+2 (90.8)
	269	0.0435	H-1 → L+1 (72.4), H-2 → L (21.4)
	257	1.0334	H-3 → L (80.4), H → L+1 (13.6)
1,7-An	443	0.0907	H → L (98.8)
	316	0.2402	H → L+1 (38.0), H-2 → L (34.6), H-1 → L (24.2)
	282	0.6042	H-2 → L (40.2), H → L+2 (35.2), H → L+1 (17.2)
	276	0.6941	H → L+2 (58.2), H-2 → L (16.4)
	253	0.6187	H-1 → L+1 (62.7), H-3 → L (15.9)
2,9-An	466	0.0885	H → L (98.9)
	349	0.0147	H → L+1 (57.2), H-1 → L (39.5)
	310	0.0772	H → L+2 (78.2), H → L+1 (10.0)
	294	1.2070	H-1 → L (48.1), H → L+1 (24.9), H → L+2 (19.5)
	261	0.0351	H-3 → L (48.7), H-2 → L (27.2), H-1 → L+1 (12.3)
	259	0.5196	H-2 → L (41.9), H-3 → L (34.0), H → L+3 (12.1)
	258	0.1274	H → L+3 (77.6), H-2 → L (14.5)
9,10-An	529	0.1029	H → L (99.3)
	371	0.2064	H → L+1 (88.1), H-1 → L (11.7)
	275	1.2451	H-1 → L (84.6), H → L+1 (11.5)
	251	0.0142	H → L+4 98.5
	224	0.0319	H → L+6 (77.9), H-1 → L+1 (17.3)
1,4-An	503	0.0727	H → L (98.9)
	353	0.1558	H → L+1 (85.4), H-2 → L (13.7)
	318	0.0205	H-1 → L (96.5)
	292	0.0457	H → L+2 (97.2)
	284	0.6672	H-2 → L (64.2), H-1 → L+1 (20.6), H → L+1 (11.3)
	252	0.1304	H-3 → L (83.4)
	241	1.2011	H-1 → L+1 (72.4), H-2 → L (15.8)

[a]For brevity, we denote the HOMO orbital as H and LUMO as L.

Table S2 Absorption wavelength (λ_{abs} in nm), oscillator strength (f_{abs}), and configuration interaction (CI) contributions (Major MO Involvement, %) of pyrene-based of diamino-substituted CDs shown in Figure 1.

model	λ_{abs}	f_{abs}	CI contribution (%)
4,9-Py	377	0.4306	H → L (93.4)
	351	0.0723	H → L+1 (81.5), H-2 → L (16.3)
	287	0.4008	H-2 → L (78.9), H → L+1 (15.8)
	249	0.3397	H-2 → L+1 (67.3), H-1 → L+2 (25.6)
	243	0.4501	H-1 → L+2 (67.6), H-2 → L+1 (20.5)
	226	0.1160	H-4 → L (87.2)
	216	1.3122	H-1 → L+3 (86.2)
1,7-Py	389	0.4064	H → L (90.9)
	364	0.0425	H-1 → L (75.6), H → L+1 (19.8)
	3151	0.0372	H → L+2 (76.7), H → L+1 (15.2)
	310	0.2216	H → L+1 (59.5), H → L+2 (20.0), H-1 → L (14.2)
	277	0.1517	H-2 → L (61.6), H-1 → L+1 (27.1)
	270	0.0647	H-1 → L+2 (87.0)
	264	0.7570	H-1 → L+1 (47.3), H-3 → L (31.2), H-2 → L (10.6)
	259	0.3159	H → L+3 (42.9), H-3 → L (34.8), H-1 → L+1 (13.1)
	247	0.1369	H → L+3 (41.4), H-3 → L (27.3), H-2 → L (13.7)
1,4-Py	397	0.3854	H → L (94.1)
	363	0.0381	H → L+1 (80.1), H-1 → L (15.0)
	321	0.2088	H-1 → L (78.6), H → L+1 (11.5)
	302	0.0817	H → L+2 (90.8)
	284	0.0465	H-2 → L (59.3), H-1 → L+1 (30.8)
	272	0.2369	H-1 → L+1 (55.2), H-2 → L (26.3)
	264	0.0825	H-3 → L (51.5), H → L+3 (28.6)
	253	0.0190	H → L+3 (53.6), H-3 → L (28.8)
	242	0.3378	H-1 → L+2 (46.0), H-2 → L+1 (33.0)
1,8-Py	411	0.4339	H → L (93.7)
	375	0.0614	H → L+1 (88.3)
	330	0.0989	H → L+2 (94.5)
	307	0.1915	H-1 → L (85.1)
	268	0.2698	H-1 → L+1 (77.8), H-3 → L (14.1)
	265	0.0753	H → L+3 (50.5), H-2 → L (35.1)
	257	0.1480	H-3 → L (82.2), H-1 → L+1 (10.5)
	252	0.0115	H-2 → L (54.3), H → L+3 (32.8)
	248	0.0141	H → L+4 (88.5)
	242	0.2698	H-1 → L+2 (67.8)

1,5-Py	423	0.3606	H $\rightarrow$ L (95.4)
	376	0.0628	H $\rightarrow$ L+1 (91.4)
	318	0.0434	H $\rightarrow$ L+2 (96.0)
	302	0.1693	H-1 $\rightarrow$ L (84.7)
	288	0.1088	H-2 $\rightarrow$ L (77.8)
	268	0.0173	H-1 $\rightarrow$ L+1 (39.7), H-3 $\rightarrow$ L (29.1), H $\rightarrow$ L+3 (22.0)
	254	0.3813	H $\rightarrow$ L+3 (54.5), H-2 $\rightarrow$ L+1 (18.0)
	251	0.0443	H-3 $\rightarrow$ L (36.2), H-2 $\rightarrow$ L+1 (29.3), H $\rightarrow$ L+3 (13.5)
	246	0.0116	H $\rightarrow$ L+4 (92.6)
	242	0.3388	H $\rightarrow$ L+5 (43.4), H-1 $\rightarrow$ L+1 (16.4), H-2 $\rightarrow$ L+1 (16.1)
	241	0.3817	H $\rightarrow$ L+5 (51.8), H-1 $\rightarrow$ L+1 (16.5)
4,5-Py	423	0.2385	H $\rightarrow$ L (94.4)
	370	0.0537	H $\rightarrow$ L+1 (90.3)
	310	0.1316	H-1 $\rightarrow$ L (91.1)
	306	0.1484	H-2 $\rightarrow$ L (74.3), H-1 $\rightarrow$ L+1 (14.1)
	293	0.0779	H $\rightarrow$ L+2 (93.3)
	257	0.4119	H-1 $\rightarrow$ L+1 (45.5), H $\rightarrow$ L+3 (36.0), H-2 $\rightarrow$ L (13.5)
	255	0.0159	H $\rightarrow$ L+4 (96.5)
	246	0.9308	H-2 $\rightarrow$ L+1 (85.4)

The molecule is divided into two fragments, i.e., amino acts as donor and the PAH core acts as acceptor. As shown in Table S3, the charge transfers mainly occur on anthracene itself when the electron is excited. A small amount of charge transfer from amino fragment to anthracene fragment. However, the charge transfer of 1,4-An is an order of magnitude larger than that of 2,3-An. As shown in Table S4, the net transfer of electrons of 1,4-An with the longest wavelength emission is also the largest. These results indicate that long-wavelength emissive CDs have a large charge transfer. The similar conclusion is found in Tables S5 and S6.

Table S3. The transfer of electrons between donor and acceptor during electron excitation of anthracene-based CDs.

2,3-An			2,7-An			1,7-An		
donor	acceptor		donor	acceptor		donor	acceptor	
	amino	anthracene		amino	anthracene		amino	anthracene
amino	0.003	0.067	amino	0.004	0.105	amino	0.006	0.157
anthracene	0.038	0.891	anthracene	0.034	0.857	anthracene	0.031	0.806
2,9-An			9,10-An			1,4-An		
donor	acceptor		donor	acceptor		donor	acceptor	
	amino	anthracene		amino	anthracene		amino	anthracene
amino	0.010	0.177	amino	0.017	0.258	amino	0.007	0.311
anthracene	0.042	0.771	anthracene	0.044	0.681	anthracene	0.015	0.667

Table S4. The net transfer of electrons between donor and acceptor during electron excitation of anthracene-based CDs.

model	amino	anthracene
2,3-An	-0.029	0.029
2,7-An	-0.071	0.071
1,7-An	-0.126	0.126
2,9-An	-0.135	0.135
9,10-An	-0.214	0.214
1,4-An	-0.295	0.295

Table S5. The transfer of electrons between donor and acceptor during electron excitation of pyrene-based CDs.

4,9-Py			1,7-Py			1,4-Py		
donor	acceptor		donor	acceptor		donor	acceptor	
	amino	pyrene		amino	pyrene		amino	pyrene
amino	0.007	0.132	amino	0.006	0.146	amino	0.007	0.158
pyrene	0.041	0.821	pyrene	0.032	0.816	pyrene	0.036	0.799
1,8-Py			1,5-Py			4,5-Py		
donor	acceptor		donor	acceptor		donor	acceptor	
	amino	pyrene		amino	pyrene		amino	pyrene
amino	0.013	0.189	amino	0.009	0.247	amino	0.004	0.315
pyrene	0.049	0.747	pyrene	0.026	0.718	pyrene	0.009	0.671

Table S6. The net transfer of electrons between donor and acceptor during electron excitation of pyrene-based CDs.

model	amino	pyrene
4,9-Py	-0.091	0.091
1,7-Py	-0.113	0.113
1,4-Py	-0.123	0.123
1,8-Py	-0.140	0.140
1,5-Py	-0.221	0.221
4,5-Py	-0.306	0.306

Table S7. The calculated absorption wavelengths (λ_{abs}, nm), absorption oscillator strengths (f_{abs}), PL emission wavelengths (λ_{em}, nm), emission oscillator strengths (f_{em}), HOMO–LUMO energy gaps (eV) of the excited state, charge transfer numbers (CT), and hole-electron contribution values of different CDs composed of polycyclic aromatic hydrocarbons (anthracene, tetracene, phenanthrene, and pyrene) and electron-donating groups ($-NH_2$, $-N(CH_3)_2$, $-OH$, $-OCH_3$, and $-CH_3$).

model	λ_{abs}	f_{abs}	λ_{em}	f_{em}	HOMO	LUMO	gap	CT	hole	electron
Anthracene	393	0.085	**461**	0.089	-5.27	-2.20	3.06	-	-	-
Pyrene	331	0.001	**342**	0.002	-5.38	-2.00	3.39	-	-	-
2,3-An-OH	395	0.073	**462**	0.079	-5.11	-2.04	3.07	0.008	**3.51%**	2.70%
2,7-An-OH	412	0.065	**488**	0.069	-5.01	-2.07	2.94	0.033	**5.31%**	2.04%
1,7-An-OH	418	0.082	**491**	0.084	-4.96	-2.04	2.92	0.053	**7.39%**	2.08%
2,9-An-OH	435	0.082	**511**	0.082	-4.86	-2.04	2.82	0.072	**9.86%**	2.62%
9,10-An-OH	462	0.085	**560**	0.079	-4.68	-2.03	2.64	0.123	**15.20%**	2.92%
1,4-An-OH	433	0.074	**528**	0.069	-4.80	-2.00	2.80	0.132	**14.88%**	1.72%
2,3-An-OCH$_3$	388	0.054	**450**	0.062	-5.05	-1.89	3.15	0.006	**4.24%**	3.60%
2,7-An-OCH$_3$	432	0.066	**508**	0.067	-4.87	-2.04	2.83	0.052	**7.74%**	2.54%
1,7-An-OCH$_3$	423	0.101	**496**	0.102	-4.86	-1.97	2.89	0.065	**9.23%**	2.69%
2,9-An-OCH$_3$	429	0.098	**503**	0.098	-4.93	-2.09	2.85	0.060	**8.55%**	2.58%
9,10-An-OCH$_3$	412	0.118	**498**	0.118	-5.03	-2.16	2.87	0.045	**7.39%**	2.93%
1,4-An-OCH$_3$	431	0.083	**526**	0.077	-4.73	-1.90	2.83	0.159	**17.88%**	2.01%
2,3-An-CH$_3$	394	0.074	**462**	0.079	-5.12	-2.06	3.06	0.005	**1.86%**	1.41%
2,7-An-CH$_3$	390	0.074	**459**	0.079	-5.13	-2.05	3.09	0.008	**1.92%**	1.17%
1,7-An-CH$_3$	394	0.094	**463**	0.098	-5.14	-2.08	3.06	0.010	**2.81%**	1.81%
2,9-An-CH$_3$	412	0.098	**484**	0.101	-5.05	-2.12	2.93	0.003	**3.66%**	3.32%
9,10-An-CH$_3$	417	0.127	**491**	0.128	-5.04	-2.14	2.89	0.020	**5.94%**	3.95%
1,4-An-CH$_3$	400	0.109	**470**	0.112	-5.15	-2.12	3.03	0.022	**4.34%**	2.16%
2,3-An-N(CH$_3$)$_2$	417	0.031	**483**	0.036	-4.82	-1.82	2.99	0.122	**17.05%**	4.87%
2,7-An- N(CH$_3$)$_2$	445	0.027	**524**	0.030	-4.44	-1.64	2.80	0.126	**18.11%**	5.51%
1,7-An- N(CH$_3$)$_2$	450	0.133	**537**	0.129	-4.46	-1.72	2.73	0.204	**25.24%**	4.82%
2,9-An- N(CH$_3$)$_2$	453	0.121	**560**	0.106	-4.41	-1.76	2.65	0.286	**33.94%**	5.37%
9,10-An-N(CH$_3$)$_2$	427	0.015	**610**	0.152	-4.39	-1.89	2.50	0.365	**42.66%**	6.18%
1,4-An- N(CH$_3$)$_2$	464	0.109	**716**	0.068	-4.03	-1.76	2.27	0.374	**40.31%**	2.96%
2,3-An-NH$_2$	408	0.054	**472**	0.060	-4.83	-1.79	3.03	0.029	**7.03%**	4.14%
2,7-An-NH$_2$	423	0.044	**508**	0.045	-4.61	-1.74	2.87	0.071	**10.93%**	3.82%
1,7-An-NH$_2$	443	0.091	**540**	0.082	-4.49	-1.76	2.73	0.126	**16.31%**	3.67%
2,9-An-NH$_2$	466	0.089	**559**	0.085	-4.36	-1.72	2.64	0.135	**18.67%**	5.20%
9,10-An-NH$_2$	529	0.103	**705**	0.079	-4.01	-1.76	2.25	0.214	**27.48%**	6.06%

1,4-An-NH$_2$	503	0.073	**785**	0.039	-3.96	-1.82	2.14	0.295	**31.76%**	2.21%
4,9-Py-NH$_2$	377	0.431	**418**	0.502	-4.83	-1.63	3.20	0.091	**13.83%**	4.74%
1,7-Py-NH$_2$	389	0.406	**431**	0.473	-4.73	-1.58	3.15	0.113	**15.13%**	3.82%
1,4-Py-NH$_2$	397	0.385	**463**	0.329	-4.59	-1.57	3.02	0.123	**16.52%**	4.26%
1,8-Py-NH$_2$	411	0.434	**476**	0.407	-4.39	-1.47	2.92	0.140	**20.21%**	6.19%
1,5-Py-NH$_2$	423	0.361	**520**	0.280	-4.31	-1.55	2.76	0.221	**25.57%**	3.51%
4,5-Py-NH$_2$	423	0.239	**538**	0.163	-4.44	-1.69	2.75	0.306	**31.93%**	1.37%
2,3-Te-NH$_2$	536	0.050	**625**	0.051	-4.57	-2.21	2.36	0.016	**4.96%**	3.41%
2,9-Te-NH$_2$	552	0.044	**664**	0.042	-4.42	-2.16	2.26	0.039	**7.23%**	3.34%
1,9-Te-NH$_2$	564	0.078	**684**	0.072	-4.43	-2.23	2.20	0.072	**10.37%**	3.16%
2,11-Te-NH$_2$	590	0.079	**710**	0.073	-4.28	-2.16	2.12	0.070	**11.99%**	5.04%
5,12-Te-NH$_2$	697	0.074	**992**	0.049	-3.90	-2.19	1.71	0.201	**24.51%**	4.45%
1,4-Te-NH$_2$	641	0.055	**1102**	0.025	-3.92	-2.29	1.63	0.278	**29.44%**	1.62%
1,6-Phe-NH$_2$	357	0.164	**401**	0.215	-4.81	-1.16	3.65	0.184	**19.92%**	1.54%
3,6-Phe-NH$_2$	366	0.038	**411**	0.047	-4.73	-1.13	3.60	0.202	**20.72%**	0.51%
1,10-Phe-NH$_2$	363	0.156	**444**	0.048	-4.75	-1.28	3.47	0.200	**22.67%**	2.65%
1,9-Phe-NH$_2$	370	0.097	**456**	0.112	-4.53	-1.23	3.31	0.222	**24.74%**	2.59%
9,10-Phe-NH$_2$	394	0.029	**493**	0.025	-4.46	-1.25	3.21	0.311	**31.41%**	0.27%
1,4-Phe-NH$_2$	399	0.172	**570**	0.115	-4.18	-1.43	2.75	0.326	**34.93%**	2.29%

Equations

Process of single-electron excitation can be described as an electron leaves hole and goes to electron. In most practical cases, excitations have to be represented as transition of multiple MO pair with corresponding weighting coefficients. Therefore, the single orbital pair representation is not suitable as HOMO→LUMO transition.

The density distribution of hole and electron be defined as

$$\rho^{\text{hole}}(r) = \sum_{i \to a}(w_i^a)^2 \varphi_i(r)\varphi_i(r) + \sum_{i \to a}\sum_{j \neq i \to a} w_i^a w_j^a \varphi_i(r)\varphi_j(r) \tag{1}$$

$$\rho^{\text{hole}}(r) = \sum_{i \to a}(w_i^a)^2 \varphi_a(r)\varphi_a(r) + \sum_{i \to a}\sum_{i \to b \neq a} w_i^a w_j^a \varphi_a(r)\varphi_b(r) \tag{2}$$

The total magnitude of charge transfer length is referred to as D index

$$D = \sqrt{(D_x)^2 + (D_y)^2 + (D_z)^2} \tag{3}$$

The H measures overall average degree of spatial extension of hole and electron distribution in X/Y/Z direction

$$H = (\sigma_{ele} + \sigma_{hole})/2 \tag{4}$$

The t index is designed to measure separation degree of hole and electron in charge transfer direction

$$t = D - H \tag{5}$$

where If t index<0, it implies that hole and electron is not substantially separated due to charge transfer. Clear separation of hole and electron distributions must correspond to evidently positive t index.

The "electron" of course carries negative charge, while "hole" can be regarded as carrying positive charge, therefore formally there is a Coulomb attractive energy between them, its negative value is known as exciton binding energy, which is a

positive value. This term can be calculated via simple Coulomb formula (in atomic unit form):

$$E_c = \iint \frac{\rho^{hole}(r_1)\rho^{ele}(r_2)}{|r_1 - r_2|} dr_1 dr_2 \qquad (6)$$

To characterize overlapping extent of hole and electron, S_r are defined as follows

$$S_r = \int S_r(r)dr = \int \sqrt{\rho^{hole}(r)\rho^{ele}(r)}dr \qquad (7)$$

The difference between RMSD of electron and hole in X/Y/Z direction can be measured via $\Delta\sigma_\lambda$, while overall difference can be measured via $\Delta\sigma$

$$\Delta\sigma_\lambda = \sigma_{ele,\lambda} - \sigma_{hole,\lambda} \qquad \lambda = \{x, y, z\} \qquad (8)$$

$$\Delta\sigma = |\sigma_{ele}| - |\sigma_{hole}| \qquad (9)$$

There are often many nodes or complicated fluctuations in hole and electron distributions. In order to make visual study of hole and electron easier, C_{hole} and C_{ele} functions are defined as follows. The function behavior of C_{hole} and C_{ele} is similar to Gaussian function, they are highly smooth functions, the value asymptotically approaches zero from centroid of hole/electron.

$$C_{ele}(r) = A_{ele} \exp(-\frac{(x-X_{ele})^2}{2\sigma^2_{ele,x}} - \frac{(y-Y_{ele})^2}{2\sigma^2_{ele,y}} - \frac{(z-Z_{ele})^2}{2\sigma^2_{ele,z}}) \qquad (10)$$

$$C_{hole}(r) = A_{hole} \exp(-\frac{(x-X_{hole})^2}{2\sigma^2_{hole,x}} - \frac{(y-Y_{hole})^2}{2\sigma^2_{hole,y}} - \frac{(z-Z_{hole})^2}{2\sigma^2_{hole,z}}) \qquad (11)$$

where the factor A is introduced so that C_{hole} and C_{ele} are normalized.

Equations 1–11 come from the manual of Multiwfn 3.7 code.[3]

References

1. K. Lee, D. Kim, *J. Phys. Chem. C* 2016, **120**, 28330–28336.

2. P. K. Samanta, D. Kim, V. Coropceanu, J. L. Bredas, *J. Am. Chem. Soc.* 2017, **139**, 4042–4051.

3. T. Lu and F. Chen, *J. Comput. Chem.*, 2012, **33**, 580–592.